Reliability-based life cycle costing analysis for embedded rails in level crossings

Shang, Yue; van den Boomen, Martine; de Man, Amy; Wolfert, Rogier

DOI
10.1177/0954409719866359

Publication date
2019

Document Version
Final published version

Published in
Proceedings of the Institution of Mechanical Engineers, Part F: Journal of Rail and Rapid Transit

Citation (APA)
Shang, Y., van den Boomen, M., de Man, A., & Wolfert, R. (2019). Reliability-based life cycle costing analysis for embedded rails in level crossings. *Proceedings of the Institution of Mechanical Engineers, Part F: Journal of Rail and Rapid Transit*, *234 (2020)*(8), 821-833. https://doi.org/10.1177/0954409719866359

Original Article

Institution of MECHANICAL ENGINEERS
Journal of RAIL AND RAPID TRANSIT

Proc IMechE Part F:
J Rail and Rapid Transit
2020, Vol. 234(8) 821–833

DOI: 10.1177/0954409719866359
journals.sagepub.com/home/pif

Reliability-based life cycle costing analysis for embedded rails in level crossings

Yue Shang[1], Martine van den Boomen[1], Amy de Man[2] and ARM (Rogier) Wolfert[1]

Abstract

Reliability-based life cycle costing analysis (LCCA) supports optimized decisions on capital and operational expenditures for engineering asset management. In addition, it allows investigation of the impact of maintenance decisions on designing the service life of assets. The application of reliability-based LCCA in railway practice is challenging, as there is limited research with regard to integrating maintenance strategies, reliability and costs especially for embedded rail systems. Therefore, in this research, an LCCA model for these embedded rail system assets has been developed, which shows the optimum between the actual reliability profile, financial parameters and maintenance policies for specific variable conditions. This model incorporates both the uncertainties associated with degradation and maintenance strategies which have been integrated into a discounted age replacement model. This model facilitates a better understanding about the interaction among life cycle cost, rail degradation and maintenance strategies for a set of variable conditions. The output supports decision making on rail replacement and/or maintenance engineering. The model is demonstrated in a case study and validated with available (real) failure data from Dutch railroad service contractors. The potential of the applicability to ballasted tracks is also demonstrated.

Keywords

Life cycle cost, reliability, rail, embedded rail system, replacement

Date received: 11 December 2018; accepted: 7 July 2019

Introduction

Life cycle costing analysis (LCCA) seeks to optimize the costs for investing, operating and maintaining the assets by taking into account all cost elements throughout the lifecycle of the assets.[1] Infrastructure assets do have disposal costs which are often included in the investment costs, as they mostly occupy a small proportion of the investment. LCCA is generally recognized as a valuable tool to support the decision making on comparing various investment alternatives and establishing optimum management policies, etc.[2]

In practice, however, the estimation of LCC of railway infrastructure is a challenging issue. The most perplexing element of the LCC is maintenance costs. The railway assets are characterized by long lifespans, during which they are subject to deterioration and a substantial amount of maintenance is required to retain their reliability. Many uncertainties involved in the operating condition, e.g. traffic density, axle loads and speed, result in varied asset degradation and associated intervention costs. Conversely, the adoption of different maintenance regimes also influences the asset degradation. The type of interventions defines its effectiveness on asset reliability, and the time of maintenance application influences the degradation patterns of the assets and timing of cash flows. Both factors eventually lead to the variation in total LCC.

In view of the interaction among costs, asset degradation and maintenance strategies, the ability to integrate the reliability analysis and maintenance modelling into LCCA will provide grounds for obtaining more accurate LCC and improving the quality of decisions made in the face of uncertainties, in which a so-called reliability-based LCCA has been stressed by many researchers.[2–7]

In railway practices, several researchers have put effort in linking the impact of rail degradation to LCCA. Zhao et al.[8] developed an LCC model for

[1]Faculty of Civil Engineering and Geosciences, Delft University of Technology, Delft, The Netherlands
[2]edilon)(sedra bv, Haarlem, The Netherlands

Corresponding author:
Martine van den Boomen, Faculty of Civil Engineering and Geosciences, Delft University of Technology, Building 23, Room 3.40, P.O. Box 5048, 2628 CN Delft, The Netherlands.
Email: m.vandenboomen@tudelft.nl

evaluating the economic life of the rails, which integrates the stochastic modelling of rail failures and the impact of maintenance actions on the occurrence of failures. Considering that the mean LCC plot does not provide any information regarding the uncertainty, Vandoorne and Gräbe[9] applied Monte Carlo simulation in Zhao's model[8] to allow the quantification of the uncertainty associated with the rail degradation and imperfect inspection. Caetano and Teixeira[10] also extended the work of Zhao et al.[8] and presented an LCC optimization model that integrates rail, ballast and sleepers degradation models for joint maintenance planning. Rahman and Chattopadhyay[11] modelled the rail failures by using non-homogeneous Poisson Process (NHPP) and incorporated it into cost modelling to inform the rail maintenance contract.

The authors all highlight the role of uncertainties regarding the asset degradation in LCCA and address them by mathematical modelling. Given the substantial contribution of maintenance costs, they mostly focus on how to obtain the most cost-effective maintenance scenario; however, cost discounting is hardly incorporated. Discounting accounts for the time value of money, which gains in importance when the long-lived assets are considered.[12,13] Future cash flows must be discounted to allow for the fair comparison of different maintenance strategies.[2,12] Moreover, the literature review indicates that the integration of the degradation modelling and LCCA lays emphasis on the conventional ballasted tracks, while the slab track structures, e.g. the embedded rail system (ERS), has not received much attention to date.

The ERS is a rail fastening system. It replaces the traditional combination of the rail, ballast and sleepers; instead, the rail is completely embedded in a concrete slab and fixated by means of an elastic poured compound which surrounds almost the entire profile of the rails except for the rail head,[14] see Figure 1. The material saving items are for reducing the use of the elastic compound and ERS strips provide elasticity for the system and control rail deflection. Slab structures like ERS have different degradation features, maintenance requirements and corresponding life cycle costs. A few cases have been found that evaluate the LCC of the (ERS) slab tracks.[15,16] However, these studies are case specific and neglect the impact of asset degradation on LCC evaluation. These cannot provide any insight into the interaction among costs, asset degradation and maintenance strategies.

The current research screens the problem in regards to one of the applications of ERS, level crossings with ERS, being employed for the mainline traffic in Dutch national railway network (named *Harmelen* level crossing/LC), and proposes a reliability-based LCC optimization model for this asset to capture the cost interaction and improve the quality of replacement decision making in the face of uncertainties. The model is developed based on specific degradation features of Harmelen LC. However, the model structure is generic and transferable to other types of rail assets as elaborated in the discussion section.

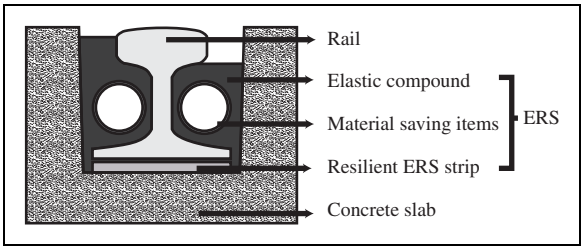

Figure 1. Structure of the slab track with ERS.

Figure 2. Level crossing with ERS (Harmelen LC, ProRail inspection photo).

This paper is organized as follows. The subsequent section presents the dominant failure modes in Harmelen LC and maintenance practices of ProRail (Dutch rail infrastructure manager). Hereafter we describe the model formulation and derive the objective cost function for replacement optimization. Next, the model applicability is demonstrated in a case study followed by a discussion of the model application for ballasted tracks. This paper is finalized with concluding remarks.

Rail degradation and maintenance practices

A rail level crossing is an intersection where a railway line and a road cross at the same level,[14] see Figure 2. It consists of two zones, i.e. the level crossing zone (where both trains and vehicles pass over) and the transition zone (the area from the ballasted track onto the slab track and from the slab onto the ballasted track). The Harmelen LC is applicable in the level crossing area and the structure in the transition zone is the ballasted track which makes a connection to the normal railway lines. One Harmelen LC basically consists of three components, namely the rail, ERS and slab.

Rail defects result from a degradation process that usually occurs as different forms of fatigue, wear, corrosion, etc. Any of these forms or their combination can become a cause of a rail break.[17] Rail breakage in this text is considered as failure and its occurrence in Harmelen LC prompts a full replacement of rail and ERS. The degradation features of the rails in Harmelen LC are elaborated in the following section.

ProRail defines the expected service life of the rails in Harmelen LC as 20 years based on all the registered Harmelen LC on the railway network. By contrast, the expected lifetime of the concrete slabs is 40 years, during which time they require less maintenance, and the associated maintenance activities (e.g. concrete injection dealing with the settlement) are less costly than the rail replacement. Therefore, practically, once, twice, or even three times the rails are replaced due to various factors without removing the concrete slabs. ERS generally has a longer lifespan than the rails but it has to be completely removed associated with rail replacement. After preparation of the concrete channels, the new rails are primed, installed and poured back in with new ERS. As a result, the lifespan of ERS in most cases depends on the rail degradation.

The rail replacement is the most influential contributor to the LCC of Harmelen LC. The current research therefore focuses on incorporating the impact of rail degradation and its associated maintenance operations in LCC modelling. ERS replacement costs are included in the rail replacement costs.

Rail defects and failure

Corrosion is the major contributor of rail degradation in Harmelen LC.[18] It can occur anywhere in the rail, especially in the area where the rail sticks out of the slab and the ballasted track continues (Figure 3). The rail in this location is more susceptible to moisture, road debris and de-icing salt. Another influencer is the local settlement in the transition zone. The slab is a rigid concrete structure and hardly causes subsidence under loads, while, with the accumulated traffic loading, the ballast gradually deteriorates and causes geometric unevenness. This differential settlement gives rise to dynamic forces when trains transit onto or off the level crossings, which in turn leads to the rotation of the rail and stresses in the elastic compound (then debonding from the rail). Water combined with road debris and salt will flow into the gaps and the corrosion starts. For better stability of the transition zone, it is prescribed that the subsoil should be well compacted to achieve the required deformation modulus and a geotextile is applied on top of that to strengthen the soil.[19] Another extra measure is a minimum of 5 to 8 solid sleepers being built in immediately after the level crossings.[19]

As observed in Figure 3, the rail head surface does not suffer from corrosion because the wear keeps it polished, and grinding (illustrated in section Inspection and maintenance) can also remove the rail surface imperfections. The problem of corrosion almost occurs in locations where the rail is not open and exposed, typically the rail foot. Limited ventilation and lack of sunlight lead to situations where water remains present in the concrete channel for a long time and its reaction with road debris and salt has a major impact on corrosion.[18]

Figure 3. Reduced profiles in rail foot caused by corrosion (ProRail inspection photo).

Rail foot corrosion in the long term leads to volume reduction of the rail foot and deterioration of the bearing capacity. This material loss at worst causes a sudden rail breakage. In many cases, the corrosion-initiated breaks are unpredictable, as the "clogging" of the rail hinders the proper inspection: rail foot corrosion at the end of level crossings (the ballast track continues) can be evaluated by visual inspection, while the segment cast in ERS is not visible. This creates a situation where the state of the rail is unclear and it further corrodes. Practically repairing the rail corrosion is not possible (only replacement), but with every new (or being replaced) level crossings, rails are now prescribed with the protective coating for lifetime extension and interference reduction.[18]

In general, instant breaks occurring in Harmelen LC do not impose safety risks, as the rails are fixated in the elastic compound which protects the whole structure from full collapse. A point of attention is the train protection system connected by the rails to continuously provide information to trains regarding their relative locations to others. The signals will disappear once a break occurs. In this case, a copper leash is used to connect the two ends and make the signal connection work again, which will influence the train speed.

Rolling contact fatigue (RCF) is another influencer of the rail degradation, which is also a significant problem in ballasted tracks.[20,21] The rail, subjected to the repeated loading cycles, is susceptible to metal fatigue.[22] Cannon et al.[22] described the development of RCF failure. A fatigue crack initiates when repeated stress with sufficient magnitude is applied to a rail section; it propagates with the repeated loading. Without any intervention the end result is rail

break. The typical RCF defects are squats and head checks, which are found on all types of tracks and mostly caused by contact stress between the rail and wheel.[20–22] The squat defect is one of the common RCF defects in Harmelen LC. Its cause manifests itself as a localized depression on the running surface of the rail head.

Inspection and maintenance

Maintenance can be generally classified into preventive maintenance (PM) and corrective maintenance (CM).[2,23] PM indicates the activities being performed prior to the system failure while CM is a strategy to repair or replace an asset after its failure.[23] Nowadays, railway asset managers tend towards PM regime as it contributes to reducing failure risks of railway tracks and preventing downtime loss. In the case of Harmelen LC, as the rail breaks/failures require a full replacement and do not impose safety risks (motivated earlier), the current study also considers CM as corrective replacement (CR) and it might cause additional costs resulting from downtime. PM and CM are balanced based on lowest life cycle costs and reliability. According to the effectiveness, maintenance actions may also be classified into three cases: perfect, minimal and imperfect.[24] Perfect maintenance restores a system to be as good as new; minimal maintenance restores a system to the same condition as just before the maintenance is performed (as bad as old); and imperfect maintenance restores a system to be worse than new but better than old.

A combination of inspection methods is generally used for detecting rail defects and failures to increase the inspection accuracy, namely non-destructive testing (NDT) (ultrasonic inspection, eddy-current inspection, etc.), visual inspection and track circuit measurements. Ultrasonic inspection is predominantly used for detecting the rail defects in Harmelen LC, carried out twice a year by ProRail. Based on the propagation of ultrasonic waves in the tested steel, it can measure the fatigue crack depth and also indicate the rail corrosion by measuring the distance between the rail head and rail foot and comparing it to the standard rail profile. It however lacks accuracy, as it cannot measure how much steel rail has been corroded. There is currently no effective and satisfying inspection technique to detect corrosion defects. Asset managers mostly rely on visual inspection to check the bonding of the elastic compound, corrosion near the rail end, etc. Besides, when it comes to RCF defects, shallow cracks in the gauge corner are difficult to check by means of ultrasound testing; typically, as shown in Figure 4, when shallow fissures occur at small angles to the upper rail surface, it is difficult to bring the ultrasound into the rail from the driving surface to crack tip.[21,25] The other issue relates to shallow crack shadowing, where small cracks block waves from reaching deeper cracks.[22]

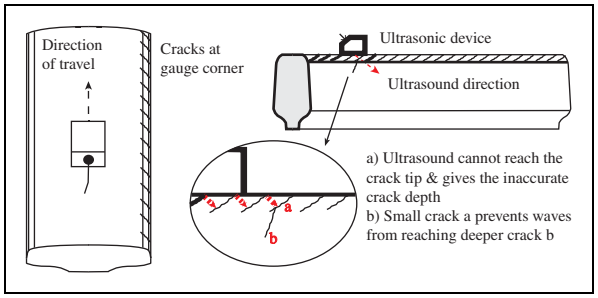

Figure 4. Unreliable detection of crack depth and shallow crack shadowing in ultrasound measurement (adapted from Edel[25]).

Grinding has been undertaken for many years to maintain the rail.[22] The emphasis has been given on its effectiveness as a treatment for RCF defects.[20,22] Grinding removes fatigue-damaged material layers from the rail running surfaces and forms an improved rail head profile. Corrosion mostly occurs at the rail foot so that grinding cannot help mitigate this problem. In this case, grinding is considered imperfect maintenance. The preventive cyclic grinding regime has been fully employed over the Dutch national railway network.[20] The rails in level crossings are ground every 15 MGT (million gross tons) with each metal removal of 0.2 mm.[26] In most cases the maximum wear allowed is 17 mm.

Both RCF and corrosion contribute to the rail degradation, while RCF defects can be detected early and its potential failures can be avoided by preventive rail replacement (severe defects) or grinding (shallow cracks). As a result, rail breaks in Harmelen LC are mostly corrosion-related. The preventive replacement (PR) decision depends on the local condition (by inspections) and asset managers. It is planned in a specific time horizon, while, once a rail breaks, an immediate/corrective action within 24 h must be performed. The rail break occurring in Harmelen LC prompts full rail replacement, and partial rail replacement by welding is not possible, because it is not allowed to have welds in Harmelen LC.[19] Besides, whether it is corrective or preventive action, the ERS needs to be fully replaced associated with the rail replacement.

Model formulation

Given the dominant maintenance operations, the cost components considered in this paper include acquisition costs, inspection costs (ultrasonic and visual), preventive grinding costs, replacement costs (preventive and corrective). Both replacement scenarios are considered perfect replacements (or repairs) as the full replacement brings the rail back into its original condition. The current research defines that one lifecycle of the rails begins with a replacement and ends just before the next replacement. After each replacement, the cycle starts all over again.

The full rail and ERS replacement result in high replacement costs. Due to the substantial contribution to the LCC, the rail replacement decision significantly influences the LCC of Harmelen LC. To find an optimized replacement interval such that the total LCC can be minimized, the age replacement model is considered.

Under an age replacement policy, the asset is replaced preventively when it reaches a predefined replacement age or correctively upon failure, whichever comes first.[2] The optimum is found by minimizing the expected cost rate per unit time $C(t_p)$, calculated as follows[27]

$$C(t_p) = \frac{\textit{Expected cost in one cycle}}{\textit{Expected cycle length } E(L)} = \frac{C_p R(\mathrm{t}_p) + C_c F(\mathrm{t}_p)}{t_p R(\mathrm{t}_p) + \mathrm{M}(\mathrm{t}_p) F(\mathrm{t}_p)} \quad (1)$$

where C_p = preventive replacement costs; C_c = corrective replacement costs; t_p = preventive replacement interval; $R(\mathrm{t})$ = reliability function; $F(\mathrm{t})$ = cumulative distribution function and $M(\mathrm{t}_p)$ = expected duration of the failure cycle defined as $M(\mathrm{t}_p) = \int_0^{\mathrm{t}_p} \frac{tf(t)\mathrm{d}t}{F(\mathrm{t}_p)}$. All symbols and units are defined in the Notation section at the end of the article.

The fundamental age replacement model assumes the maintenance operations to be perfect. In the railway case, preventive grinding is imperfect as it is not effective in dealing with corrosion failure. The replacement optimization should consider its impact on controlling the RCF defects and possibility of extending the rail's service life, where the extension of the age replacement model is needed. The proposed model goes through three stages, as presented in Figure 5.

Reliability modelling

Several papers addressed the occurrence of rail failures in ballasted tracks to be governed by a 2-parameter Weibull distribution,[8,10,14,22,28] and the stochastic modelling of rail degradation to be represented by a Weibull hazard rate $h(t)$, as defined in equation (2).[29]

$$h(t) = \frac{\beta}{\alpha}\left(\frac{t}{\alpha}\right)^{\beta-1} \quad (2)$$

where α and β are the well-known Weibull scale and shape parameters. Appendix 1 provides a full description of the Weibull distribution.

The Weibull law however is found in ballasted tracks. It is unknown whether it is applicable to Harmelen LC. The model therefore starts with failure data gathering.

In step 1, two forms of failure data are considered, namely exact failure times and interval data. The latter originates from the situation where the exact failure times of one system cannot be observed and only intervals are known. As the corrosion and RCF are two distinct failure modes, the failure data are separated.

Step 2 applies probability plotting to select a reliability model and determine its goodness-of-fit. Since every rail failure requires a full replacement, the rail in Harmelen LC is considered as non-repairable and life distributions are suitable candidates to model its failure times. As the commonly used distribution for modelling the rail failures in the ballasted tracks, the Weibull distribution is firstly chosen to graphically test the model fit with regression analysis (least squares fit). The coefficient of determination (R^2) is chosen as a goodness-of-fit measure. Benard's median

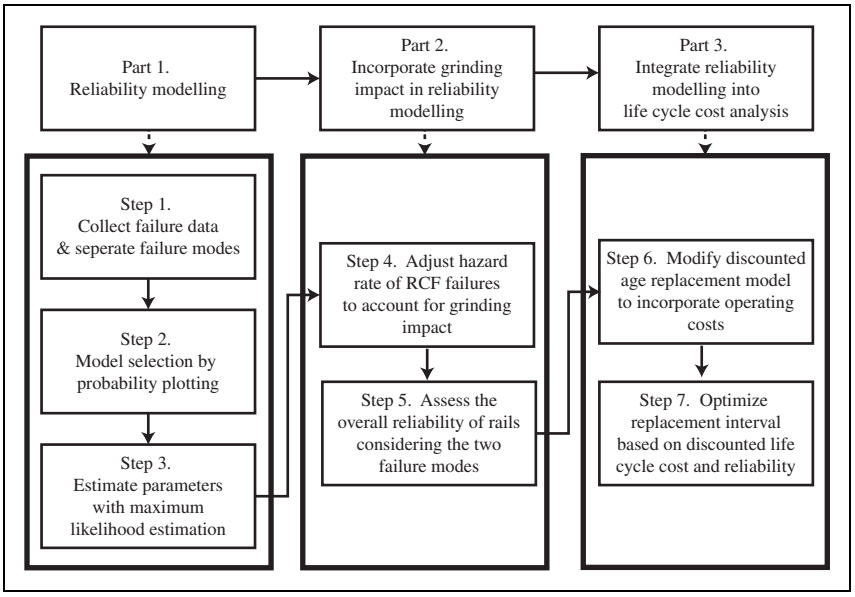

Figure 5. Flowchart of the reliability-based LCC model.

rank estimate[30] is used for exact failure times and binomial estimate is for interval data.[29] For the readers' convenience, a description is provided in Appendix 2.

In step 3, maximum likelihood estimation (MLE) is proposed to provide parameter estimates of the fitted distribution. Statisticians prefer MLE over other estimates as the former in general has better statistical characteristics, especially for a large dataset.[29,31] Appendix 3 provides a description of the MLE. This study numerically solves the MLE in Excel. The result is presented in the section Application.

Modelling of grinding impact

The grinding cycles are planned based on local tonnage, while practically asset managers integrate the annual tonnage of track lines (in MGT), grinding frequency (in months) and metal removal of one pass (in mm), and use time frequency to inform the grinding implementation.[26] For example, in case that the annual tonnage is 15 MGT and grinding cycle is once per 12 months, one-time metal removal is 0.2 mm. The depth of metal removal should be adapted to time variation of actual implementation (if the grinding operations are early performed or delayed). The research sets 15 MGT equal to 12 months of train operation as an average to incorporate the impact of cyclic preventive grinding in rail degradation modelling and explore how the grinding policy influences the LCC.

To evaluate the performance of imperfect maintenance, generally the hazard rate of the system under maintenance is used.[8,11,32] Coria et al.[32] proposed a (periodic) PM optimization model, where the impact of PM on asset degradation is included by adjusting the hazard rate. This study incorporates it in the model (step 4) in order to evaluate the effect of grinding frequency on the rail degradation and LCC optimization.

Assume the grinding is performed at fixed intervals T_{pm} and the time of the k^{th} grinding is $t_k = kT_{pm}, k = 1, 2, \ldots, N$, where N is the number of grinding operations within one replacement cycle T and $t_{N+1} = T$. As shown in Figure 6, $\lambda_k(t)$ is the hazard rate of RCF-initiated failure at time t after the k^{th} grinding, where $0 \leqslant t < T_{pm}$. Its fluctuation is caused by the periodic grinding operation. Coria et al.[32] proposed a hypothetic hazard rate which smooths the original hazard rate by including T_{pm} as a parameter. These two functions define the same area under the curves, i.e., the same expected number of rail failures within a replacement cycle.[32] Finally, the authors derived the adjusted Weibull hazard rate $h(t,\ T_{pm})$ as follows, comparable to equation (2).

$$h(t,\ T_{pm}) = \left(\frac{T_{pm}}{T_0}\right)^{\beta} \frac{\beta}{\alpha}\left(\frac{t}{\alpha}\right)^{\beta-1} \tag{3}$$

where T_0 is the current grinding interval.

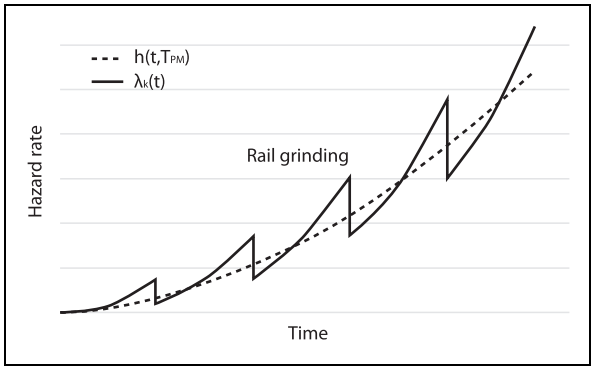

Figure 6. Comparison of the (real) hazard rate and adjusted hazard rate (adapted from Coria et al.[32]).

Step 5 evaluates the overall reliability of the rails considering the two failure modes. Assume the corrosion and RCF are independent and the rails are at risk from either failure mode. Here the rails are considered as series systems, where an important notion is: a single component with several independent failure modes is analogous to a system with several independent components.[29] Following the series system probability argument, the total hazard rate of rail failures $h_s(t)$ is calculated as[29]

$$h_s(t) = h_1(t) + h_2(t) = \frac{\beta_1}{\alpha_1}\left(\frac{t}{\alpha_1}\right)^{\beta_1-1} + \left(\frac{T_{pm}}{T_0}\right)^{\beta_2} \frac{\beta_2}{\alpha_2}\left(\frac{t}{\alpha_2}\right)^{\beta_2-1} \tag{4}$$

Integrate reliability modelling into LCCA

Step 6 extends the age replacement model to incorporate the expenditures used for routine maintenance, i.e. grinding, ultrasonic inspection and visual inspection, where the sum is considered as the operating costs. Assume the activities are carried out at fixed intervals, the cumulative operating costs $C_o(t_p)$ incurred in $[0, t_p]$ are calculated as

$$C_o(t_p) = C_{pm} \cdot \frac{t_p}{T_{pm}} + C_{ui} \cdot \frac{t_p}{T_{ui}} + C_{vi} \cdot \frac{t_p}{T_{vi}} \tag{5}$$

where C_{pm} = costs of one-time grinding operation; C_{ui} = costs of one-time ultrasonic inspection; C_{vi} = costs of one-time visual inspection. T_{ui} = ultrasonic inspection interval and T_{vi} = visual inspection interval.

Under the age replacement policy, the incurrence of the operating costs is influenced by the rail failures. Defining the PR interval as t_p, if a failure occurs before t_p, e.g. $t(0 < t \leqslant t_p)$, the operating costs are incurred in the failure replacement cycle $[0, t]$; if no failure occurs in $[0, t_p]$, the operating costs are incurred in the full PR cycle. The weighted average

of operating costs is a product of probabilities of the two possible replacement cases with the associated operating costs. The extended age replacement model is therefore expressed as

$$C(t_p) = \frac{\left\{ \begin{array}{l} C_c \cdot F(t_p) + C_p \cdot R(t_p) + \int_0^{t_p} C_o(t) \cdot f(t)\mathrm{d}t \\ \quad + C_o(t_p) \cdot \mathrm{R}(t_p) \end{array} \right\}}{t_p R(\mathrm{t_p}) + \mathrm{M}(\mathrm{t}_p) F(\mathrm{t}_p)} \tag{6}$$

Van den Boomen et al.[12] proposed an LCC approach for including the time value of money in the fundamental age replacement model (equation (1)), which combines three common economic factors, i.e. present worth factor $\alpha(t)$, annuity factor $(A/P, r, t)$, and capitalized equivalent worth (CW) factor. The present worth factor represents straightforward discounting and is defined as $\alpha(t) = 1/(1+r)^t$ where r is the annual discount rate and t is the time. The annuity factor transforms a present value into equal annual costs over a life cycle t by multiplying this present value with $(A/P, r, t) = r(1+r)^t/[(1+r)^t - 1]$. The CW factor is used to transform a present value into an infinite stream of equivalent annual cost (EAC). This factor is obtained by letting t approach to infinity in the annuity factor and simply results in discount rate r. These factors will be used in the following discounted LCC modelling.

Step 7 applies the methodology for cost discounting in the extended model (equation (6)). This paper considers discrete discounting on a monthly basis and the following equations change the continuous probability distribution (equation (6)) to discrete distribution, where $\sum_{t=0}^{t_p} f(t) = F(t_p), f(t)$ is assumed to be 0 at time zero.

The numerator of equation (6) expresses the total maintenance costs over $[0, t_p]$. Its PV, denoted as PV_m, is calculated as

$$\mathrm{PV}_m = C_c \cdot \sum_{t=1}^{t_p} f(t)\alpha(t) + C_p \cdot R(t_p) \cdot \alpha(t_p) + \mathrm{PV}_o \tag{7}$$

The first expression on the right side designates the discounted expected costs of a corrective replacement, the second expression designates the discounted expected costs of a preventive replacement and PV_o represents the discounted expected total operating costs in interval $[0, t_p]$, calculated as

$$\begin{aligned} \mathrm{PV}_o &= C_{o,d}(t_p) \cdot R(t_p) + \sum_{t=1}^{t_p} C_{o,d}(t) \cdot F(t) \\ &= \left[\sum_{t=1}^{t_p} C_{om}(t)\alpha(t) \right] \cdot R(t_p) + [C_{om}(1)\alpha(1)] \cdot F(1) \\ &\quad + [C_{om}(1)\alpha(1) + C_{om}(2)\alpha(2)] \cdot F(2) \\ &\quad + \cdots + \left[\sum_{t=1}^{t_p} C_{om}(t)\alpha(t) \right] \cdot F(t_p) \end{aligned}$$

where $C_{o,d}(t_p) =$ discounted cumulative operating costs and $C_{om}(t) =$ monthly operating costs in time t without discounting.

The annuity factor, $(A/P, r, t)$, converts a PV to EAC over a life cycle t. EAC here is interpreted as the equivalent monthly cost (EMC) because of the monthly discounting, where the monthly discount rate, i, is used. The annuity factor is therefore denoted as $(A/P, i, t)$. This step converts the PV_m (equation (7)) to the EMC over the expected cycle length $E(L)$ which is defined by the denominator of equation (1), by the annuity factor where t equals to $E(L)$ (equation (8)).

$$EMC_{E(L)} = PV_m \cdot (A/P, i, E(L)) \tag{8}$$

When t approaches infinity, the limit of $(A/P, i, t)$ is i.[33] Assuming t approaches infinity means assuming perpetual life and repeated replacements, where EMC is a constant equivalent cash flow regardless of the number of life cycles, so that $\mathrm{EMC}_{E(L)} = \mathrm{EMC}_\infty$. This typical characteristic of EMC (or EAC in general) allows for comparison of EMC values when alternatives have unequal lives as is by definition the case in optimization challenges where the replacement interval is a variable.

Moreover, there is still a one-time initial investment at $t = 0$ with probability 1 which has to be considered and translated into an EMC value for comparison. This first investment is not yet included in equation (7). Equation (7) only accounts for successive repetitive investments from t_p onwards. The CW approach is used to calculate the EMC_∞ of this initial investment: the initial investment costs (C_{in}) are equally distributed over infinity and the EMC of the initial investment costs is calculated as

$$\mathrm{EMC}_{in} = C_{in} \cdot i \tag{9}$$

Combining equations (8) and (9), the total EMC (the sum of maintenance and investment costs) over infinity is obtained

$$\mathrm{EMC}_{total} = \mathrm{EMC}_{E(L)} + \mathrm{EMC}_{in} \tag{10}$$

Equation (10) is an objective cost function that links the impact of rail degradation and maintenance decision variables ($t_p, t_{pm}, t_{ui}, t_{vi}$) to LCC. The minimum of EMC_{total} provides an economic optimum for supporting the replacement decision.

Application

In this section, the model for replacement optimization is applied to an ERS case study. Field data and

cost information are collected from ProRail, Strukton and ASSET Rail. Maintenance policies refer to ProRail's practices.

Twenty-one rail breaks (in four years) that occurred in Harmelen LC of ProRail's network are collected. It was found that nearly all the rail failures were caused by corrosion. One of the reasons is the RCF defects can be detected and prevented early and the exact times of potential RCF-initiated rail failures can hardly be observed.

ProRail defines four severity levels of rail defects and corresponding time horizons for preparing the PR activities. Generally, the defect diagnosis and replacement decisions are recorded on the ultrasonic inspection report. It is proposed to combine the ultrasonic inspection data with expert judgment on the question, "starting from the inspection date (when the RCF defect is defined to a certain level), how long can the rail stand before it breaks, considering 'do nothing' scenario?" For instance, if the time frame from the level 2 to the potential failure occurrence is one year and the age of the rail when it is inspected is 20 years, it is possible to infer that the potential rail failure caused by the recorded defect may occur during the 240th–252nd month. This kind of failure data refers to interval data.

Due to the inadequacy of the ultrasonic inspection data, this paper assumes the time intervals (Table 1a) where RCF failures may occur based on the 20-year expected rail life (defined by ProRail as stated before) to demonstrate the model application. The estimates start on month 180 as it assumes no RCF-initiated failure occurs before that time. The varied number of failures in the same time interval is caused by the different local operating conditions (including environmental factors) of Harmelen LC, e.g. tonnage, train speed, humidity, road debris, that influence the rail degradation. Since corrosion is the dominant rail failure mode in Harmelen LC, the 20-year average is mostly influenced by the problem of corrosion and the rails when solely considering RCF failure mode may stand longer than the average 20 years. Therefore, in the estimation, within the same time interval (20 months, i.e. duration of the intervals 220th–240th, 240th–260th months, etc.), the maximum four RCF-initiated failures are estimated in the interval 280th–300th rather than the intervals around the 20-year average (interval 220th–240th, 240th–260th).

The corrosion failure mode is modelled by field data, as presented in Table 1b, where 19 (corrosion-related) out of 21 failure times are used. The registration starts on the 163rd month as no failure caused by corrosion occurs before that time.

The maintenance decision variables are fixed as $T_0 = 12$ months, $T_{pm} = 12$ months (reference scenario), $T_{ui} = 6$ months, $T_{vi} = 12$ months.

Figure 7 presents the Weibull probability plotting of corrosion failure data. The dots represent the sample data. It is observed that the plotted points appear to be linear. Regression analysis shows $R^2 = 0.965$, indicating the Weibull distribution provides a good fit to the given data. The regression line is $y = 4.137x - 23.729$, which provides the parameter estimates as presented in Table 2. Similarly, the RCF failure data are plotted, as shown in Figure 7 (squares); the regression line is $y = 7.397x - 41.945$. R^2 equal to 0.997 indicates the good model fit of the Weibull distribution.

Table 1. Failure data.

(a) Estimated RCF failure data (month).

Interval start	Interval end	Failures in intervals
180	200	1
200	220	1
220	240	2
240	260	2
260	280	3
280	300	4
300	320	3
320	340	1
340	360	1

(b) Registered corrosion failure data (month)

Failure count i	Failure times t_i	Failure count i	Failure times t_i
1	222	11	296
2	163	12	379
3	237	13	163
4	365	14	308
5	281	15	440
6	268	16	320
7	224	17	331
8	224	18	300
9	187	19	300
10	339		

RCF: rolling contact fatigue.

Table 2 presents the parameter values solved by least squares (LS) and MLE. As the MLE is usually a recommended approach,[29] Weibull estimates provided by MLE are used in the following steps.

In steps 4 and 5, substitute α_1 and β_1 in equation (2); α_2 and β_2 in equation (3); the overall reliability of the rails is assessed by equation (4). The cumulative hazard function is calculated by integrating the total hazard rate. The other functions of the Weibull distribution are derived with their relations to the cumulative hazard function (see details in Appendix 1).

In steps 6 and 7, considering an 18-m long Harmelen LC, the following financial parameters are fixed (Table 3). The difference between C_p and C_c lies in the social costs and indirect costs. The social costs

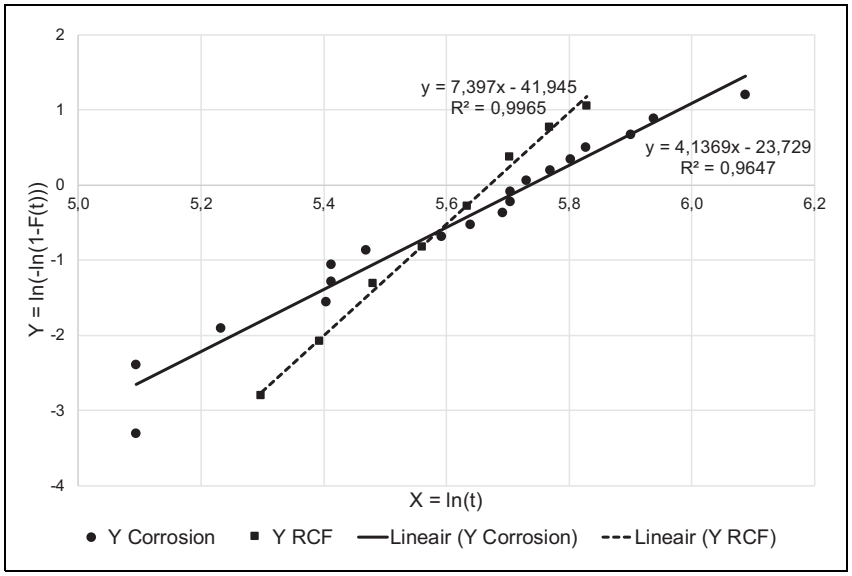

Figure 7. Weibull probability plot of corrosion and RCF failure data.

Table 2. Comparison of LS and ML estimators.

Failure mode	Weibull parameters	Least squares estimation	Maximum likelihood estimation
Corrosion	α_1	309.845	309.272
	β_1	4.137	4.280
RCF	α_2	290.177	289.720
	β_2	7.397	7.619

RCF: rolling contact fatigue.

measure the economic impact of track unavailability in case of failures and its cost elements represent the average level in the Netherlands.

Substituting the result of reliability modelling, fixed maintenance variables and financial parameters in equations (5) and (6) and following the discounting procedures (equations (7) to (10)) yields the bold black reference curve in Figure 8. This curve represents the total EMC curve versus the PR interval. The EMC curve expresses the EMC for each PR interval at the x-axis and balances the costs of a preventive replacement with the costs of a probable corrective replacement. For example, the black curve shows the EMC for all life cycles induced by preventive replacements of the scenario with the 12-month grinding interval. At first, the EMC curve will decline as a consequence of a very small probability for a rail break and subsequent corrective replacement. The EMC curve will reach an optimum and increase again because the probability of the failure costs increases as the life cycle increases. At a certain life cycle the probability of a failure will be 1. Hereafter, the EMC curve will become constant but this will not have a physical meaning as a broken rail will not be left broken.

The teeth on the EMC curve are caused by periodically incurred operating costs (grinding and inspections). Note that EMC is not the amount of total costs over a lifecycle but the costs per unit time, which is used for cost comparison and replacement optimization, i.e. compare LCC with different PR policies (associated with different expected lifecycles) and advise to the optimized PR interval at minimized EMC.

The modelling yields an optimized PR interval, 179 months (15 years), where the EMC_{total} is minimized as 556. It is interpreted as, given the rail degradation, maintenance policies and financial parameters, if one asset manager decides to preventively replace the rail when it reaches the 15th year (in case no failure occurs in that period) or correctively replace the rail upon failure (and the next PR is scheduled after 15 years), the asset manager is able to own the asset at the minimized costs.

The above optimum is found by fixing t_{pm} as 12 months. Figure 8 also presents the total EMC curves under six grinding scenarios. It is observed that the more frequent grinding operations postpone the economic optimum for the PR interval, as the grinding is effective in controlling the RCF degradation and by cost tradeoff the model advises to preventively replace the rails later.

The calculation of the mean time to failure (MTTF) indicates the impact of grinding on the rail reliability: when $T_{pm} = 16$, MTTF = 16years; when $T_{pm} = 6$, MTTF = 23years. Moreover, Figure 9 presents the hazard rate graph under different grinding scenarios. When $T_{pm} = T_0 = 12$, equation (3) is simplified to the basic form of Weibull hazard rate (equation (2)). Taking the curve ($T_{pm} = 12$) as a baseline, it is obvious that with more frequent grinding operations, the hazard rate only shows a slight increase

Table 3. Financial parameters.

Financial parameters	Values	Remarks
Annual discount rate (r)	5%	
Monthly discount rate (i)	0.407%	$i = (1 + r)^{\frac{1}{12}} - 1$
Investment (C_{in})	€40,000	
Preventive replacement (C_p)	€36,000	€30,000 for single rail replacement; additional 20% for indirect cost
Social cost (C_s)	€69,632	Unit cost of track availability 17/h/passenger Average number of passengers 128 passengers/train Average number of trains 4 trains/h Unavailability duration 8 h (fault duration 12 h minus free night possession time 4 h)
Corrective replacement (C_c)	€108,632	€30,000 for single rail replacement; additional 30% for indirect cost; social cost included
Preventive grinding cost (C_{pm})	€2000	One-time operation cost for an 18-m long Harmelen LC
Ultrasonic inspection cost (C_{ui})	€200	
Visual inspection (C_{vi})	€300	

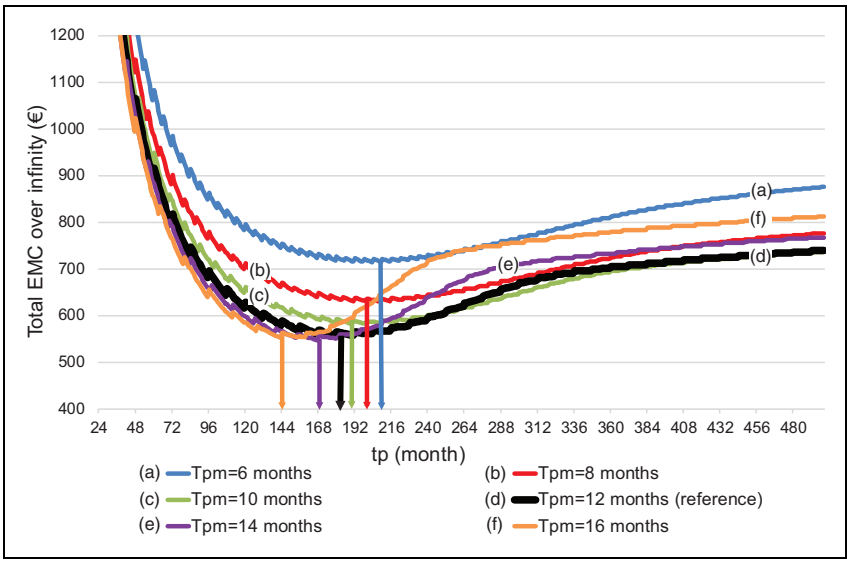

Figure 8. Total EMC and replacement optimization with different grinding frequencies.

over time. By contrast, when $T_{pm} = T_0 = 12$, the hazard rate dramatically increases.

Discussion

Due to the non-repairable feature of the ERS, the lifetime of the rails is taken as a random quantity and the Weibull distribution is applied to account for the randomness of the rail failures. The life distributions assume that the time to failure is a sample of independent and identically distributed (i.i.d.) observations. In the literature, some assume that the arrivals of rail failures follow NHPP. The rail breaks in the ballasted tracks can be repaired by partial rail replacement. In its lifecycle, several rail failures may occur and a trend may exist in the failure times, as each subsequent failure depends on the actions taken for rectifying the previous failures. The NHPP focuses on the interarrival times of failures.

In the railway practices, whether to choose the Weibull distribution or NHPP for modelling the rail failures depends on the i.i.d. premise. The first task in rail reliability modelling is to test against this assumption. It also sheds light on the model applicability to the ballasted tracks. In this paper, the repeated replacement, life distribution and perpetual annuity ($\mathrm{EMC}_{E(L)} = \mathrm{EMC}_{\infty}$) share the i.i.d. assumption. Whether the assumption holds is the key to justify the model used for the ballasted tracks. In the test against the i.i.d., "test for trend" is generally performed to check whether the times between failure follow a common distribution; and "test for serial correlation" is applied to check for independence. Once the assumption is verified given the failure

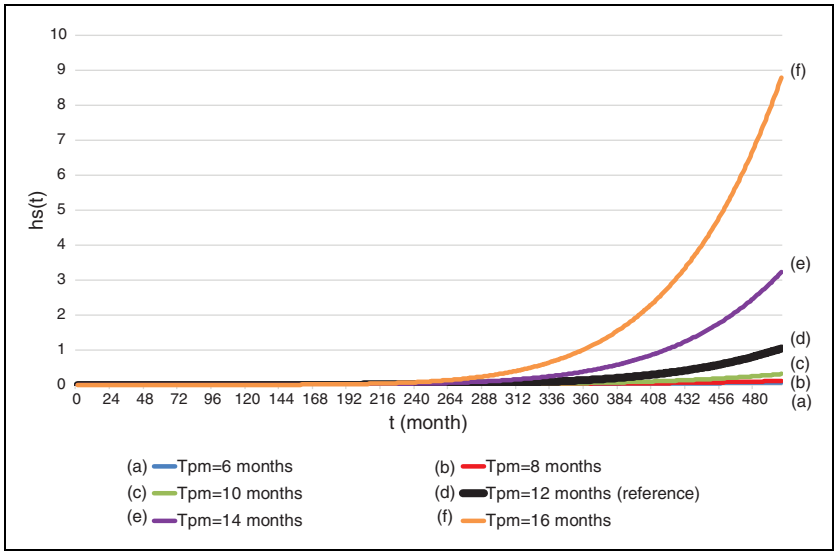

Figure 9. Impact of grinding frequencies on the total hazard rate of rail failures.

data, the reliability modelling can be connected to the proposed model.

An observation worth mentioning is that an optimal maintenance regime should minimize the LCC of the assets without compromising its safety. The elastic compound in the ERS allows for (accidental) CR as it protects the structure from full collapse in the case of a rail break. Rail assets which are not allowed to fail can also be modelled with the same age replacement model; however, in those cases the CR costs are modelled as extremely high, due to the impact of failure. Alternatively, the dominant optimization objective is set as reliability instead of costs. In general, the age replacement model allows for optimizing replacement intervals based on a (combined) cost or reliability objective.

Conclusions and future work

This paper developed an empirical LCC optimization model for the embedded rails in Harmelen LC. The applicability to the ballasted tracks was elaborated. The model incorporates the uncertainties involved in the rail degradation and maintenance policies by integrating the reliability analysis and maintenance modelling to a discounted age replacement model.

The model yields an optimal time interval to inform the decision maker on the average preventive rail replacement of Harmelen LC. It builds on current best knowledge of a reliability profile, financial parameters and maintenance policies for specific variable conditions. The model demonstrates a significant role of grinding frequencies on extending the service life and replacement of rails. As the corrosion-initiated rail breaks are difficult to predict and the model includes estimated RCF failure data, it is recommended to validate the model by gathering more feedback data like NDT inspection reports and break records from the Harmelen LC service.

This paper assumes the independency between the corrosion and RCF failure modes. Future research could incorporate the interaction, i.e. explore how the random failure times caused by the failure modes are correlated and integrate its impact to LCCA to improve the quality of replacement decisions. Besides, the current study uses time as an indicator to model the randomness of rail failures. Future extensions can investigate the impact of the operating factors, e.g. traffic tonnage, train speed, curvature, on the rail degradation and adapt the model to different operation conditions. Also, it is worth studying the interactive effect of rail degradation with ERS and the adjacent ballasted track to improve the structural design and life cycle management.

Acknowledgements

The authors would like to thank ProRail, ASSET Rail and Strukton for offering rail failure and inspection data and sharing maintenance policies.

Declaration of Conflicting Interests

The author(s) declared no potential conflicts of interest with respect to the research, authorship, and/or publication of this article.

Funding

The author(s) received no financial support for the research, authorship, and/or publication of this article.

ORCID iD

Martine van den Boomen https://orcid.org/0000-0002-5040-7680

References

1. Ammar M, Zayed T and Moselhi O. Fuzzy-based life-cycle cost model for decision making under subjectivity. *J Constr Eng Manag* 2012; 139: 556–563.

2. Sánchez-Silva M and Klutke G-A. *Reliability and life-cycle analysis of deteriorating systems*. Basel: Springer, 2016.
3. Saad L, Aissani A, Chateauneuf A, et al. Reliability-based optimization of direct and indirect LCC of RC bridge elements under coupled fatigue-corrosion deterioration processes. *Eng Fail Anal* 2016; 59: 570–587.
4. Tee KF, Khan LR, Chen HP, et al. Reliability based life cycle cost optimization for underground pipeline networks. *Tunnel Undergr Space Technol* 2014; 43: 32–40.
5. Frangopol DM, Kong JS and Gharaibeh ES. Reliability-based life-cycle management of highway bridges. *J Comput Civil Eng* 2001; 15: 27–34.
6. Kong JS and Frangopol DM. Life-cycle reliability-based maintenance cost optimization of deteriorating structures with emphasis on bridges. *J Struct Eng* 2003; 129: 818–828.
7. Kong JS and Frangopol DM. Cost–reliability interaction in life-cycle cost optimization of deteriorating structures. *J Struct Eng* 2004; 130: 1704–1712.
8. Zhao J, Chan AHC, Roberts C, et al. Assessing the economic life of rail using a stochastic analysis of failures. *Proc IMechE, Part F: J Rail and Rapid Transit* 2006; 220: 103–111.
9. Vandoorne R and Gräbe PJ. Stochastic modelling for the maintenance of life cycle cost of rails using Monte Carlo simulation. *Proc IMechE, Part F: J Rail and Rapid Transit* 2018; 232: 1240–1251.
10. Caetano LF and Teixeira PF. Optimisation model to schedule railway track renewal operations: a life-cycle cost approach. *Struct Infrastruct Eng* 2015; 11: 1524–1536.
11. Rahman A and Chattopadhyay G. Modelling cost of maintenance contract for rail infrastructure. In: *Proceedings of the 2010 International Conference on Industrial Engineering and Operations Management*, Dhaka, Bangladesh, 9–10 January, 2010. IEOM Society International.
12. van den Boomen M, Schoenmaker R and Wolfert A. A life cycle costing approach for discounting in age and interval replacement optimisation models for civil infrastructure assets. *Struct Infrastruct Eng* 2018; 14: 1–13.
13. van den Boomen M, Schoenmaker R, Verlaan J, et al. Common misunderstandings in life cycle costing analyses and how to avoid them. In: *Proceedings of the 5th international symposium on life-cycle civil engineering*. Milton Park: Taylor & Francis Group, 2017.
14. Esveld C. *Modern railway track*. Zaltbommel: MRT-Productions, 2001. Retreived from: http://www.esveld.-com/Documents/MRT_Selection.pdf
15. Gailienė I and Laurinavičius A. The need and benefit of slab track: case of Lithuania. *Gradevinar* 2017; 69: 387–396.
16. Zoeteman A and Esveld C. Evaluating track structures: life cycle cost analysis as a structured approach. In: *World Congress on Railway Research*, Tokyo, 1999.
17. Shafiee M, Patriksson M and Chukova S. An optimal age–usage maintenance strategy containing a failure penalty for application to railway tracks. *Proc IMechE, Part F: J Rail and Rapid Transit* 2016; 230: 407–417.
18. Valkenburg C. Technical research and LCM analysis preservation methods (Technisch onderzoek en LCM-analyse conserveringsmethoden: ProRail gaat spoorstaven conserveren. Civiele Techniek nummer 7). *Civiele Techniek* 2015; Thema Geotechniek. Uitgeverij SJP Uigevers, pp. 2–3.
19. ProRail. *Level crossing with heavy type Harmelen (Overweg met zware overwegplaten type Harmelen)*. Utrecht: ProRail, 2010.
20. Zoeteman A, Dollevoet R and Li Z. Dutch research results on wheel/rail interface management: 2001–2013 and beyond. *Proc IMechE, Part F: J Rail and Rapid Transit* 2014; 228: 642–651.
21. Popović Z, Radović V, Lazarević L, et al. Rail inspection of RCF defects. *Metalurgija* 2013; 52: 537–540.
22. Cannon D, Edel KO, Grassie S, et al. Rail defects: an overview. *Fatigue Fract Eng Mater Struct* 2003; 26: 865–886.
23. Ahmad R and Kamaruddin S. An overview of time-based and condition-based maintenance in industrial application. *Comput Ind Eng* 2012; 63: 135–149.
24. Blischke WR and Murthy DP. *Reliability: modeling, prediction, and optimization*. New York: John Wiley & Sons, 2000.
25. Edel K-O. International symposium 'rail defects' (Internationales Symposium 'Schienenfehler'). *Interdisciplinary research network railway engineering (Interdisziplinärer Forschungsverbund Bahntechnik)*. Brandenburg: University of Applied Sciences Brandenburg, 2000.
26. NeTIRail. Practices and track technology tailored to particular lines (Deliverable 2.2). In: RESEARCH A-E (ed) *Collaborative project H2020-MG-2015-2015 GA-636237, Needs Tailored Interoperable Railway – NeTIRail-INFRA*, 2015. Retrieved from: https://ec.europa.eu/research/participants/documents/download Public/R1hEK2NtRUpBR21HaDlpRDFqQnJNZl greTgrN0NPbDNqbFdiK052dXdXZUxxdzhMQjEx-N0ZBPT0 = /attachment/VFEyQTQ4M3ptUWNwYT RrQ1R1RmFZSEtpbXFRa2tXRzk =
27. Jardine AK and Tsang AH. *Maintenance, replacement, and reliability: theory and applications*. Boca Raton: CRC Press, 2013.
28. Liu X, Lovett A, Dick T, et al. Optimization of ultrasonic rail-defect inspection for improving railway transportation safety and efficiency. *J Transp Eng* 2014; 140: 04014048.
29. Tobias PA and Trindade D. *Applied reliability*. Boca Raton: CRC Press, 2011.
30. Benard A and Bos-Levenbach E. *The plotting of observations on probability-paper*. Stichting Mathematisch Centrum. Statistische Afdeling, 1955.
31. Elmahdy EE. A new approach for Weibull modeling for reliability life data analysis. *Appl Math Comput* 2015; 250: 708–720.
32. Coria V, Maximov S, Rivas-Dávalos F, et al. Analytical method for optimization of maintenance policy based on available system failure data. *Reliab Eng Sys Saf* 2015; 135: 55–63.
33. Sullivan WG, Wicks EM, Koelling CP, et al. *Engineering economy*. New York: Pearson/Prentice Hall/Pearson Education International, 2012.

Appendix

Notation

C_c corrective replacement cost [currency]

$C(t_p)$	expected cost rate per unit time [currency/unit time]
$C_o(t)$	cumulative operating cost incurred in [0, t]; [currency]
$C_{o,d}(t)$	discounted cumulative operating cost incurred in [0, t]; [currency]
$C_{om}(t)$	monthly operating cost in time t without discounting; [currency]
C_p	preventive replacement cost [currency]
C_{pm}	cost of one-time grinding for a (defined length) Harmelen LC [currency]
C_{ui}	cost of one-time ultrasonic inspection for a (defined length) Harmelen LC [currency]
C_{vi}	cost of one-time visual inspection for a (defined length) Harmelen LC [currency]
CW	capital equivalent worth; $CW = \frac{EMC}{i}$
$E(L)$	expected cycle length [unit time]; denominator of equation (1)
$f(t)$	probability distribution function (PDF); $\int_0^{t_p} f(t)\mathrm{d}t = F(t_p)$
$F(t)$	cumulative distribution function (CDF); $F(t) = 1 - R(t)$
$h(t)$	Weibull hazard rate
$h_s(t)$	total hazard rate of rail failures, equation (4)
$h_1(t)$	hazard rate of corrosion failure mode, equation (2)
$h_2(t)$	hazard rate of RCF failure mode, equation (3)
i	monthly discount rate; $i = (1+r)^{\frac{1}{12}} - 1$
$M(t_p)$	expected length of the failure cycle [unit time]
r	annual discount rate
$R(t)$	reliability function
t	lifetime (time to failure) of the rail [unit time]; $t > 0$
t_p	preventive replacement interval [unit time]
T_0	current grinding interval [unit time]
T_{pm}	grinding interval variable [unit time]
T_{ui}	ultrasonic inspection interval [unit time]
T_{vi}	visual inspection interval [unit time]
α	Weibull scale parameter; $\alpha > 0$
α_1	Weibull scale parameter (corrosion)
α_2	Weibull scale parameter (RCF)
$\alpha(t)$	present worth factor at time t; $\alpha(t) = \frac{1}{(1+i)^t}$
β	Weibull shape parameter; $\beta > 0$
β_1	Weibull shape parameter (corrosion)
β_2	Weibull shape parameter (RCF)
$(A/P, i, t)$	annuity factor; $(A/P, i, t) = \frac{i(1+i)^t}{(1+i)^t - 1}$

Appendix 1. Weibull distribution

Hazard function: $h(t) = \frac{\beta}{\alpha}\left(\frac{t}{\alpha}\right)^{\beta-1}$
Cumulative hazard function: $H(t) = \left(\frac{t}{\alpha}\right)^{\beta}$
PDF: $f(t) = \frac{\beta}{\alpha}\left(\frac{t}{\alpha}\right)^{\beta-1} e^{-\left(\frac{t}{\alpha}\right)^{\beta}} = h(t) \cdot e^{-H(t)}$
CDF: $F(t) = 1 - e^{-\left(\frac{t}{\alpha}\right)^{\beta}} = 1 - e^{-H(t)}$
Reliability function: $R(t) = e^{-\left(\frac{t}{\alpha}\right)^{\beta}} = e^{-H(t)}$

Appendix 2. Probability plotting

Taking natural logarithms of Weibull CDF twice, the Weibull linear transformed CDF is given by

$$\ln\{-\ln[1 - F(t)]\} = \beta \ln t - \beta \ln \alpha$$

If the Weibull distribution holds, the plot of $\ln\{-\ln[1 - F(t)]\}$ versus $\ln t$ on linear axes should result in data points that approximately form a straight line, with slope β and intercept b (i.e. $-\beta \ln \alpha$). $F(t)$ is estimated from the sample data, which is called empirical CDF, $\hat{F}(t)$. The following are two estimates for deriving $\hat{F}(t)$.

Benard's median rank estimate is expressed as[30]

$\hat{F}(t_i) = \frac{i-0.3}{n_1+0.4}$ $i = 1, 2, 3, \ldots$, where t_i = time to the ith failure and $t_i \geqslant t_{i-1}$; n_1 = total number of exact failure times.

Binomial estimate: let $T_i (i = 1, 2, 3 \ldots)$ denote a fixed time interval and d_i be the number of failures in the i^{th} interval, i.e. (T_{i-1}, T_i), the binomial estimate at the k^{th} interval $\hat{F}(T_k)$ is[29]

$\hat{F}(T_k) = \frac{\sum_{i=1}^{k} d_i}{n_2}$ $i = 1, 2, 3, \ldots,$ where $n_2 =$ total number of failures in the interval data.

Appendix 3. Maximum likelihood estimation

Given the data, MLE attempts to find the parameter values that maximize the likelihood (LIK) function. The LIK function varies depending on the type of failure data. The observations that have exact failure times t_i contribute to the form PDF, $f(t_i)$, to the LIK function. As for the Weibull distribution, LIK is written as

$$\mathrm{LIK}(\alpha, \beta) = \prod_{i=1}^{n_1} f(t_i) = \prod_{i=1}^{n_1} \frac{\beta}{t_i}\left(\frac{t_i}{\alpha}\right)^{\beta} e^{-\left(\frac{t_i}{\alpha}\right)^{\beta}}$$

For interval data, where failures occur in an interval, $(T_{i-start}, T_{i-end})$ contributes the form $[F(T_{i-end}) - F(T_{i-start})]$ in the LIK equation. The LIK for the Weibull distribution is defined as

$$\begin{aligned}\mathrm{LIK}(\alpha, \beta) &= \prod_{i=1}^{r} [F(t_{i-end}) - F(t_{i-start})] \\ &= \prod_{i=1}^{r} \left\{ \left[1 - e^{-\left(\frac{t_{i-end}}{\alpha}\right)^{\beta}}\right] - \left[1 - e^{-\left(\frac{t_{i-start}}{\alpha}\right)^{\beta}}\right] \right\}\end{aligned}$$

To obtain the "most likely" values that maximize the LIK functions, the common way is to take natural logarithm of the LIK, i.e. log LIK, and numerically solve for a minimum.